Colloids and Surfaces B: Biointerfaces 121 (2014) 99–105

Contents lists available at ScienceDirect

Colloids and Surfaces B: Biointerfaces

journal homepage: www.elsevier.com/locate/colsurfb

Redox targeting of DNA anchored to MWCNTs and TiO_2 nanoparticles dispersed in poly dialyldimethylammonium chloride and chitosan

Ali A. Ensafi[a,*], Parisa Nasr-Esfahani[a], Esmaeil Heydari-Bafrooei[b], B. Rezaei[a]

[a] Department of Chemistry, Isfahan University of Technology, Isfahan 84156–83111, Iran
[b] Department of Chemistry, Faculty of Science, Vali-e-Asr University of Rafsanjan, P.O. Box 518, Rafsanjan, Iran

ARTICLE INFO

Article history:
Received 24 January 2014
Received in revised form 24 May 2014
Accepted 28 May 2014
Available online 4 June 2014

Keywords:
DNA-based biosensors
Multiwall carbon nanotubes
TiO_2 nanoparticles
Methylene blue
Electrochemical method

ABSTRACT

A key issue associated with electrochemical DNA-based biosensors is how to enhance DNA immobilization on the substrates. In order to improve the immobilization of DNA and to optimize DNA interaction efficiency, different kinds of strategies have been developed. In this regard, nanomaterials have attracted a great deal of attention in electrode surface modification for DNA biosensor fabrication. In this study, nanostructured films were deposited at the surface of a pencil graphite electrode (PGE) as a working electrode. For the present purpose, common polyelectrolytes are used for surface modification with double-stranded DNA. Two positively charged polyelectrolyte, namely poly dialyldimethylammonium chloride (PDDA) and chitosan, are initially compared for DNA immobilization at the surface of MWCNTs and TiO_2 nanoparticles (TiO_2NPs). In a second step, the basic electrochemical properties of the sensors are investigated using voltammetric methods. The modified electrodes are also characterized by scanning electron microscopy and electrochemical impedance measurements. It will be shown that electrode modification with DNA and the nanostructure that disperses in PDDA leads to an enhanced sensitivity of the DNA voltammetric detection mechanism. In a previous study, a comparison was done between MWCNTs and TiO_2NPs for determining the effect of nanoparticle effect on DNA immobilization on the electrode surface. In order to compare the efficiency of the prepared DNA-based biosensors, methylene blue is chosen as an electroactive probe. It will be shown that the stability of the immobilized DNA within several days will be much higher when MWCNTs rather than TiO_2NPs are used.

1. Introduction

Sequence-specific detection of nucleic acid targets has become increasingly important in disease diagnostics, drug screening, epidemic prevention, and environmental protection [1]. So far, many techniques including spectrophotometry [2], chemiluminescence [3], phosphorescence [4], fluorescence [5], chromatography [6], and electrochemical methods [7,8] have been developed for DNA determination. In recent years, the development of DNA biosensors has received great attention due to its extreme importance in many fields, such as clinical diagnostics [9], gene therapy [10], environmental monitoring [11], food safety [12], and biological research [13]. DNA recognition layers can be combined with electrochemical transducers to form new and important types of biosensors [14]. Electrochemical DNA biosensor technologies have been developed due to their several advantages, such as high sensitivity, good selectivity, low cost, rapid diagnosis, and the possibility of miniaturization [15].

DNA-based electrochemical sensors exploit a range of different chemistries, but all take advantage of nanoscale interactions between the target in solution, the recognition layer, and a solid electrode surface. Numerous approaches to electrochemical detection have been developed, including direct electrochemistry of DNA, electrochemistry at polymer-modified electrodes, electrochemistry of DNA-specific redox reporters, electrochemical amplifications with nanoparticles, and electrochemical devices based on DNA-mediated charge transport chemistry [16]. Recently, an impressive number of inventive designs have appeared for DNA-based electrochemical sensing. These types of sensors combine the nucleic acid layer with electrochemical transducers to produce a biosensor that expectedly provide a simple, accurate, and inexpensive platform for clinical diagnosis [17]. Electrochemical methods are well suited for DNA diagnostics. Because electrochemical reactions give an electronic signal directly, there is no need for inexpensive signal transduction equipment. Moreover, because immobilized probe sequences can be readily confined to a variety

* Corresponding author. Tel.: +98 311 3912351; fax: +98 311 3912350.
E-mail addresses: aaensafi@gmail.com, Ensafi@cc.iut.ac.ir (A.A. Ensafi).

http://dx.doi.org/10.1016/j.colsurfb.2014.05.040
0927-7765/

of electrode substrates, detection can be accomplished with an inexpensive electrochemical analyzer. Sensitive electrochemical signaling strategies based on the direct or catalyzed oxidation of DNA bases, as well as the redox reactions of reporter molecules or enzyme recruited to the electrode surface by specific DNA probe target interactions and by charge transport reactions mediated by the π-stacked base pairs have all been demonstrated [18].

Surface immobilization of DNA plays an important role in the performance of DNA biosensors. The amount of immobilized DNA probe will directly influence the accuracy, sensitivity, selectivity, and life of a DNA biosensor [19]. The development of nanomaterials for the immobilization of DNA has attracted great attention over the past decades in fabricating electrochemical DNA biosensors [20,21]. Because of their high surface-to-volume ratio and excellent biological compatibility, nanomaterials can enlarge the sensing surface area that greatly increases the amount of immobilized DNA, while the DNA mixed with nanomaterials can satisfactorily maintain its biological activity. The nanomaterials used in DNA biosensors include nanoparticles, nanowires, and nanotubes like carbon nanotubes (CNTs), among others [19].

As one of the most promising nanomaterials in photochemistry and biochemistry, nano-titanium dioxide (TiO_2) acts as an efficient agent in biosensing applications due to its good intrinsic biocompatibility, specific affinity to biomolecules, and high reactivity [22,23]. Owing to its high conductivity and low cost, TiO_2 has become an attractive electrode material in its different forms such as nanoparticles, nano-needles and nanotubes for fabricating electrochemical DNA-based biosensors [24]. The properties of CNTs, such as high electronic conductivity and high mechanical resistance, have also led to their use in the preparation of electrochemical sensors [25]. DNA is an important biological polymer, which is classified as a natural, negatively charged polyelectrolyte due to its phosphate groups. It can be immobilized onto CNTs and TiO_2 via covalent and noncovalent interactions. However, the results are unsatisfactory because negatively charged CNTs and TiO_2 repulse the negatively charged DNA. To overcome this problem, nanoparticles are usually dispersed on such positively charged polyelectrolytes as poly dialyldimethyl ammonium chloride (PDDA) or chitosan [26].

The study of the interactions between drugs and DNA is a relatively little known area which forms an attractive field, which is essential for gaining a deeper understanding of the mechanisms of interaction and developing efficient methods for detecting these mechanisms. The knowledge thus gained will be used for designing new, efficient drugs and for their in vitro screening [27]. Some studies have demonstrated that DNA damage, which may occur by induction of DNA hypomethylation and generation of reactive oxygen species [28,29]. Induction of oxidative damage (oxidative stress) is a noticeable event to explain metal-induced mutagenicity and genotoxicity. Various carcinogenic metals such as cobalt, chromium, lead, mercury, and copper cause redox reactions in living systems [29]. These metals can produce the reactive oxygen species and reactive nitrogen species in vivo and vitro systems in experimental and clinical medicine [30–32].

In this study, to improve the immobilization of ds-DNA on the surface, a mixture of nanomaterials and positively charged polyelectrolytes was immobilized at the surface of a pencil graphite electrode (PGE). At first, two positively charged polyelectrolytes, namely poly dialyldimethylammonium chloride (PDDA) and chitosan, were compared for DNA immobilization at the surface of MWCNTs and titanium dioxide nanoparticles (TiO_2NPs). In another study, a comparison was made between MWCNTs and TiO_2NPs in order to recognize the effect of nanoparticle on DNA immobilization at the electrode surface. In order to investigate the efficiency of the prepared PGE in the determination ds-DNA and small molecules interactions, methylene blue was chosen as a model. The interaction between methylene blue and guanine bases of ds-DNA is well known in the literature [33–35]. The interaction between methylene blue and ds-DNA has generally been investigated by means of the oxidation peak current value of methylene blue [36,37]. However, we investigated the interaction between methylene blue and ds-DNA by means of the changes in the oxidation peaks current of guanine and adenine bases (of the ds-DNA) on PGE. These studies were carried out using differential pulse voltammetry technique.

2. Experimental

2.1. Chemicals

All solutions were prepared using reagent grade chemicals and doubly distilled water was used through the work. Double-stranded salmon sperm DNA (ds-DNA, catalog No. D8899) was purchased from Sigma (St. Louis, USA). Reagent grade Tris–HCl, CH_3COOH, CH_3COONa, H_3PO_4, EDTA, NaCl and NaOH were purchased from Aldrich Chemicals (Milwaukee, USA). Chitosan was obtained from Acros Chemical. Their solution was prepared by dissolving a certain amount of chitosan in 10 mL CH_3COOH (120.1 mg mL^{-1}) containing 29.2 mg mL^{-1} NaCl by aid of sonication for 30 min. PDDA (low molecular weight) were purchased from Sigma. Aqueous solutions of PDDA were initially prepared with 29.2 mg mL^{-1} NaCl. Multiwall carbon nanotubes (MWCNTs) powder (diameter 70–100 nm, length 5–9 μm) was obtained from Fluka. Titanium dioxide nanoparticles (TiO_2NPs) powder (30 nm) was obtained from Fluka. Their suspensions were prepared in chitosan and PDDA solutions after sonication for 3 h to obtain a homogeneous suspension.

2.2. Apparatus

Electrochemical measurements were performed using an Autolab PGSTAT 12, potentiostat/galvanostat connected to a three-electrode cell, Metrohm, Model 663 VA stand, with a GPES 4.9 software package (Eco Chemie, The Netherlands). The raw data was treated using the Savitzky and Golay filter (level 2) of the GPES software, followed by the GPES software moving average baseline correction with a "peak width" of 0.01. The reference electrode was Ag/AgCl and the counter electrode was a platinum wire. A standard one-compartment three-electrode cell of 20 mL capacity was used in all experiments. PGE was the working electrode. A Noki pencil was used as a holder for Pentel graphite leads. Electrical contact with the lead was obtained by soldering a metallic wire to the metallic part. The pencil was hold vertically with 12 mm of the lead extruded outside (9 mm of which was immersed in the solution). The pencil leads were used as received. All the electroanalytical measurements were performed at room temperature.

2.3. Functionalization and purification of MWCNTs

MWCNTs were purified and functionalized as described elsewhere [38]. A mass of 120 mg of MWCNTs was stirred in 10 mL of a 190.0 mg mL^{-1} nitric acid solution for 20 h. The solid product was collected on a filter paper and washed several times with distilled water until the filtrate solution became neutral (pH 7.0). The functionalized MWCNTs thus obtained were then dried in an oven at 80 °C for 24 h. Nitric acid usually causes a significant destruction of carbon nanotubes and introduces –COOH groups at the ends or at the sidewall defects of the nanotube structure.

2.4. Preparation of the modified electrodes

A preliminary chemical modification of the PGE surface was used to enhance the electrode conductivity, and to form an interface with sites for the immobilization of DNA. The films of the electrode modifier were formed via the adsorption method represented by an accumulation of species without any faradaic process. After electrochemical treatment of PGE, the surface of the PGE became functionalized. Such pretreatments are believed to result in an increase in surface quinone and other functional groups. These groups lead to further and better absorption of biomolecules, nanoparticles, and polymers on the PGE. They can also catalyze the oxidation/reduction of the analyte [39]. For this purpose, the surface of the PGE was pretreated at +1.40 V for 300 s in a quiescent solution (20 mL) of 30.0 mg mL^{-1} acetate buffer containing 1.2 mg mL^{-1} NaCl (pH 4.8). The PGEs obtained after the treatment was designated as PPGE in this study.

2.4.1. DNA/PGE

The pretreated PGEs (PPGEs) were dipped into a ds-DNA solution (1.0 mg mL^{-1} buffered with Tris–HCl, pH 7.0) for approximately 30 min and allowed to dry for 1 h at room temperature.

2.4.2. DNA/PDDA/PGE

The PPGEs were immersed into a 1.0 mg mL^{-1} PDDA solution (containing 29.2 mg mL^{-1} NaCl) for 2 h. The electrodes were then dried at room temperature before they were dipped into the ds-DNA solution (1.0 mg mL^{-1} buffered with Tris–HCl, pH 7.0) for approximately 30 min and allowed to dry for 1 h at room temperature.

2.4.3. DNA/chitosan/PGE

The PPGEs were immersed into a 1.0 mg mL^{-1} chitosan solution (containing 29.2 mg mL^{-1} NaCl) for 1.5 h. The electrodes were subsequently dried for 8 h at room temperature before they were dipped into the ds-DNA solution (1.0 mg mL^{-1} buffered with Tris–HCl, pH 7.0) for approximately 30 min and allowed to dry for 1 h at room temperature.

2.4.4. DNA/MWCNTs/PGE

The PPGEs were immersed into a 1.0 mg mL^{-1} MWCNTs suspension (containing 29.2 mg mL^{-1} NaCl without PDDA and chitosan) for 2 h. They were dried at room temperature and subsequently dipped into the ds-DNA solution (1.0 mg mL^{-1} buffered with Tris–HCl, pH 7.0) for approximately 30 min and allowed to dry for 1 h at room temperature.

2.4.5. DNA/TiO_2NPs/PGE

This modified electrode was prepared as DNA/MWCNTs/PGE. The difference lies in the use of 1.0 mg mL^{-1} TiO_2NPs suspension (containing 29.2 mg mL^{-1} NaCl without PDDA and chitosan) rather than MWCNTs.

2.4.6. DNA/MWCNTs-PDDA/PGE

The PPGEs were immersed into a 1.0 mg mL^{-1} MWCNTs (dispersed in 1.0 mg mL^{-1} PDDA solution containing 29.2 mg mL^{-1} NaCl) for 2 h. The electrodes were subsequently dried at room temperature prior to being dipped into the ds-DNA solution (1.0 mg mL^{-1} buffered with Tris–HCl, pH 7.0) for approximately 30 min. Finally, they were allowed to dry for 1 h at room temperature.

2.4.7. DNA/TiO_2NPs-PDDA/PGE

This modified electrode was prepared as DNA/MWCNTs-PDDA/PGE. In this case, a 1.0 mg mL^{-1} TiO_2NPs suspension (dispersed in 1.0 mg mL^{-1} PDDA solution containing 29.2 mg mL^{-1} NaCl) was used instead of MWCNTs.

2.4.8. DNA/MWCNTs-chitosan/PGE

The PPGEs were immersed into the 1.0 mg mL^{-1} MWCNTs (dispersed in 1.0 mg mL^{-1} chitosan solution containing 29.2 mg mL^{-1} NaCl) for 2 h and the electrodes were dried at room temperature. They were subsequently dipped into the ds-DNA solution (1.0 mg mL^{-1} buffered with Tris–HCl, pH 7.0) for approximately 30 min and allowed to dry for 1 h at room temperature.

2.4.9. DNA/TiO_2NPs-chitosan/PGE

This modified electrode was prepared as DNA/MWCNTs-chitosan/PGE using a 1.0 mg mL^{-1} TiO_2NPs suspension (dispersed in 1.0 mg mL^{-1} chitosan solution containing 29.2 mg mL^{-1} NaCl) rather than MWCNTs.

2.4.10. DNA/MWCNTs-TiO_2NPs-PDDA/PGE

The PPGEs were immersed into a suspension containing 1.0 mg mL^{-1} MWCNTs and TiO_2NPs dispersed in 1.0 mg mL^{-1} PDDA for 2 h. After drying at room temperature, the electrodes were dipped into the ds-DNA solution (1.0 mg mL^{-1} buffered with Tris–HCl, pH 7.0) for approximately 30 min and subsequently allowed to dry for 1 h at room temperature.

2.5. Procedure

Before the first measurement, the DNA–modified electrode was immersed in the acetate buffer solution (pH 4.8) for 5 min under stirring. Immediately, the voltammetric stripping step was performed by employing a positive-going differential pulse potential scan (from 0.40 to 1.40) using a pulse amplitude of 50 mV for a modulation time of 0.05 s, and a step potential of 8 mV in the blank solution (the acetate buffer pH 4.8 containing 1.2 mg mL^{-1} NaCl). The oxidation signals of guanine and adenine were recorded. The raw data were then treated using the Savitzky and Golay filter (level 2) of the GPES software followed by the GPES software moving average baseline correction using a "peak width" of 0.01. The procedure was repeated using a new PGE.

2.6. Optimizations

The optimum amount of MWCNTs (dispersed in PDDA and chitosan) on PGE was studied to obtain the guanine signal. The amount of MWCNTs in MWCNTs–PDDA and MWCNTs–chitosan composites was varied between 0.5 and 2.0 mg mL^{-1} (Fig. S1). It was observed that the oxidation peak current of guanine increased with increasing MWCNTs content up to 1.0 mg mL^{-1} before it leveled off. Therefore, 1.0 mg mL^{-1} of MWCNTs was selected and used in all the following experiments. The other optimized parameters were adopted from similar parameters in our previous studies [38,40,41].

Supplementary Fig. S1 can be found, in the online version, at http://dx.doi.org/10.1016/j.colsurfb.2014.05.040.

3. Results and discussion

3.1. SEM images of the modified electrodes

SEM is an excellent tool for studying the surface morphology of thin films on the nano-/micro-scale. Representative SEMs of the modified working electrodes are shown in Fig. 1. The surface roughness of the unmodified PGE is clearly seen in Fig. 1A. The graphite layers are quite conspicuous in this figure. From the electrode coverage morphology, it can be seen that the effective surface area of the modified working electrodes significantly increased when

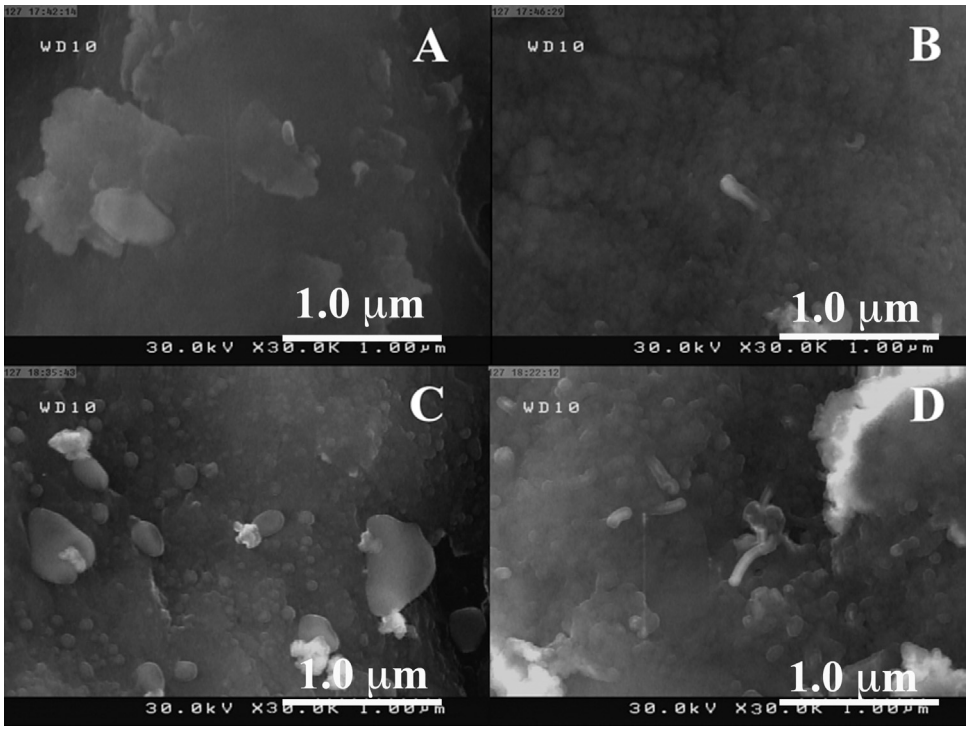

Fig. 1. SEM images of (A) PGE, (B) PDDA–MWCNTs/PGE, (C) PDDA–TiO_2NPs/PGE, and (D) Chitosan–MWCNNTs/PGE.

the highly conductive MWCNTs and TiO_2NPs were used. The SEM images of PDDA–MWCNTs (Fig. 1B), chitosan–MWCNT (Fig. 1C), and PDDA–TiO_2 (Fig. 1D) films show a homogeneous surface and good dispersion. When MWCNTs and TiO_2 were sonicated and incubated in the PDDA and chitosan solution, the positively charged polyelectrolyte PDDA and chitosan were adsorbed (or wrapped) at the surface of MWCNTs and chitosan, resulting in positively charged PDDA–and chitosan–modified MWCNTs and TiO_2. This uniform and interdigitated structure provided a significant increase in the effective area for ds-DNA loading. The negatively charged DNA made it suitable for incorporation in positively charged surfaces to form DNA modified PG electrodes.

3.2. Oxidation of ds-DNA

Different tests were performed to examine the electrochemistry of ds-DNA under various electrode conditions. The conditions for the immobilization and oxidation experiments of ds-DNA at the surface of PGE are discussed elsewhere [40,41]. The guanine and adenine bases of ds-DNA can oxide at the surface of carbon electrodes at anodic potentials in acidic media [42]. This oxidation process is used in the detection of small molecules those interact with the ds-DNA. Under the experimental conditions, the redox behavior of original ds-DNA immobilized PGE exhibited two oxidation processes of guanine (ca. +1.02 V) and adenine (ca. +1.28 V) residues. Figs. 2 and 3 show the oxidation differential pulse signals of guanine and adenine obtained at the different modified PGE. The relationship between the type of polyelectrolyte and the oxidation peaks current of ds-DNA can be seen in these two figures. When PDDA was used as the dispersant of MWCNTs (Fig. 2) and TiO_2NPs (Fig. 3), the oxidation currents of guanine and adenine bases of ds-DNA increased. On the other hand, the oxidation peaks current of guanine and adenine bases of ds-DNA at the surface of ds-DNA/PDDA–MWCNTs/PGE and ds-DNA/PDDA–TiO_2NPs/PGE increased by about 3.5 and 1.7 times vs. ds-DNA/chitosan–MWCNTs/PGE and ds-DNA/chitosan–TiO_2NPs/PGE, respectively. It was found that the electrode modification with DNA and the nanostructure that dispersed in PDDA led to the enhanced sensitivity of DNA voltammetric detection. The increase in the guanine moiety response at ds-DNA/PDDA–MWCNTs/PGE and ds-DNA/PDDA–TiO_2NPs/PGE is of interest for DNA detection. It is expected that the obvious increase in the detecting signal of guanine (or adenine) base of ds-DNA is due to the enhanced immobilization of DNA in the case of ds-DNA/PDDA–MWCNTs/PGE and ds-DNA/PDDA–TiO_2NPs/PGE. The positively charged PDDA and chitosan cover the surfaces of MWCNTs and TiO_2NPs by electrostatic interaction. The polyelectrolyte molecules can combine considerably well with DNA to form DNA films. The MWCNTs and TiO_2NPs not only display unique electron transfer properties that induce the conductivity of PDDA and improve the electron transfer characteristics, but they also increase the amount of PDDA and chitosan deposited on the electrode.

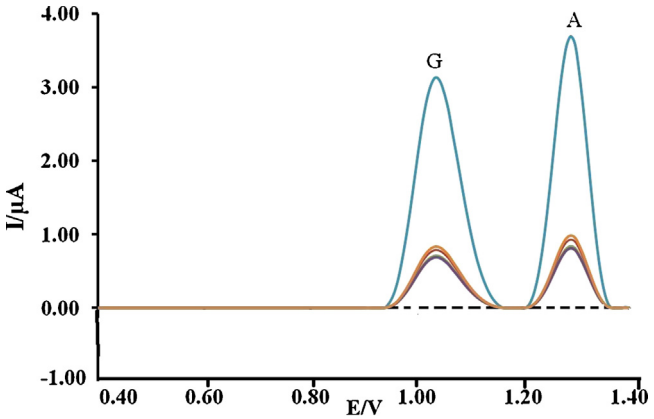

Fig. 2. Differential pulse voltammograms (from down to up) for PGE/Chitosan/ds-DNA, PGE/ds-DNA, PGE/PDDA/ds-DNA, PGE/MWCNTs/ds-DNA, PGE/Chitosan–MWCNTs/ds-DNA and PGE/PDDA–MWCNTs/ds-DNA. The dashed line (– – –) represents the DPV of a bare PGE. Conditions: scanning potential between +0.40 and +1.40 V in the acetate buffer (pH 4.8).

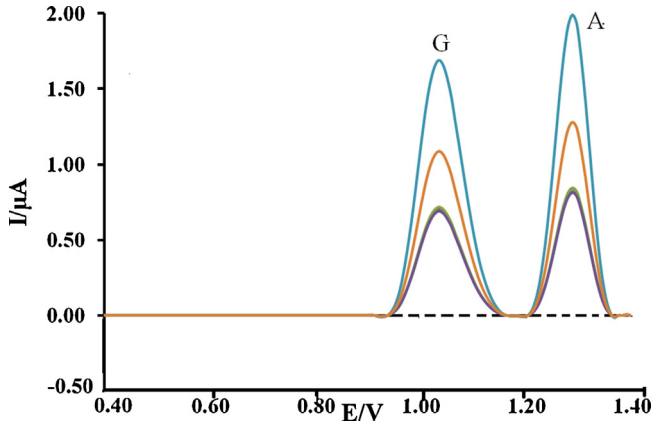

Fig. 3. Differential pulse voltammograms (from down to up) for PGE/Chitosan/ds-DNA, PGE/ds-DNA, PGE/PDDA/ds-DNA, PGE/TiO_2NPs/ds-DNA, PGE/Chitosan–TiO_2NPs/ds-DNA and PGE/PDDA–TiO_2NPs/ds-DNA. The dashed line (– – –) represents the DPV of a bare PGE. Conditions: scanning potential between +0.40 and +1.40 V in the acetate buffer (pH 4.8).

Fig. 4 shows the relationship between the type of nanomodifier and the oxidation peaks current of ds-DNA. Regarding the PGEs covered with nanomodifiers, the oxidation peaks current of adenine and guanine show an increase at both MWCNTs and TiO_2NPs. In the case of ds-DNA/PDDA–TiO_2NPs/PGE, DNA binds firmly via complexation of its phosphate group to the surface exposed titanium ions. The mesoporous morphology of the TiO_2NPs layers endows them with a huge internal contact area offering the possibility to greatly increase the amount of immobilized DNA on the substrate [43]. In the case of ds-DNA/PDDA–MWCNTs/PGE, individual DNA bases were stabilized on MWCNTs through mainly weak van der Waals interaction to the graphitic CNTs wall. This interaction is perturbed by the sugar and phosphate groups in the DNA backbone, the counter ions that bind to DNA, and the water molecules from the solution. Subsequently, the robust helical structure is formed by wrapping DNA around MWCNTs. The bases in the DNA are almost fixed in geometry and bound on the MWCNTs through mainly van der Waals attraction and the hydrophobic effect [44]. Thus, the amperometric responses obtained with the ds-DNA/PDDA–MWCNTs/PGE and ds-DNA/PDDA–TiO_2NPs/PGE prove that modification of the electrode with MWCNTs and TiO_2NPs allows the DNA immobilization capacity and sensitivity to increase so that the oxidation current of guanine and adenine increase compared to those of ds-DNA/Chitosan–MWCNTs/PGE and ds-DNA/PDDA–MWCNTs/PGE when a mixture of MWCNTs TiO_2NPs is used to construct ds-DNA/PDDA–MWCNTs–TiO_2NPs/PGE (Fig. 4). This offers an attractive prospect for using such films in DNA damage assays and DNA–molecule interactions.

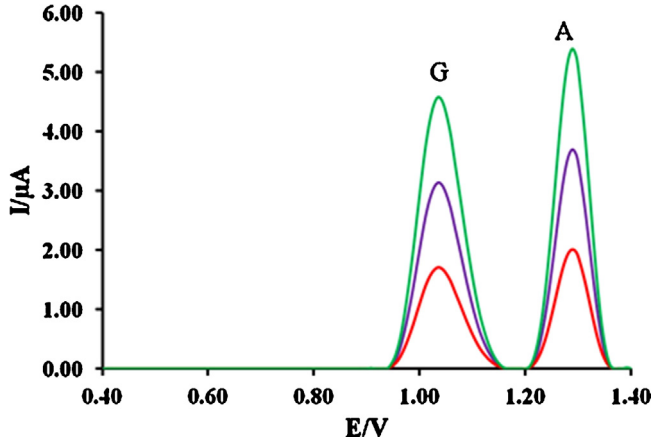

Fig. 4. Differential pulse voltammograms (from down to up) for PGE/PDDA–TiO_2NPs/ds-DNA, PGE/PDDA–MWCNTs/ds-DNA and PGE/PDDA–MWCNTs–TiO_2NPs/ds-DNA. The dashed line (– – –) represents the DPV of a bare PGE. Conditions: scanning potential between +0.40 and +1.40 V in the acetate buffer (pH 4.8).

3.3. Effect of accumulation time on the oxidation peaks current

The amount of analyte accumulated on the film coating is a function of the distribution coefficient, concentration of the analyte in the matrix and volume of the film. Therefore, the accumulation time of the ds-DNA is a very important parameter for obtaining higher guanine oxidation signals. It can be seen in Fig. 5A that the oxidation peak current of guanine and adenine bases of ds-DNA on the PDDA–MWCNTs–TiO_2NPs/PG surface increased by up to 30 min of the accumulation time. At this accumulation time, the sites of the film surface were filled with the analyte and no more ds-DNA diffused to the film surface. It may be concluded from these results that the optimum accumulation time for the ds-DNA immobilization on the PDDA–MWCNTs–TiO_2NPs/PGE is 30 min.

3.4. Effect of the ds-DNA concentration on the oxidation peaks current

To check the effect of ds-DNA concentration on the oxidation peaks current of guanine and adenine (Fig. 5B), experiments were performed in solutions with varying ds-DNA concentrations. A linear relationship was observed to exist between ds-DNA concentration and the values of the oxidation peaks current for guanine and adenine bases in a concentration range of 0.05 and 2.0 mg mL^{-1}. When the ds-DNA concentration was increased from 0.05 to 1.0 mg mL^{-1}, the linearity of the graph vanished. The slopes of the lines obtained for guanine and adenine bases of ds-DNA were very close to each other, indicating that a correlation in the oxidation peaks current. The detection limit for the ds-DNA based on guanine and adenine oxidation peaks current as estimated from S/N = 3 was obtained to be 10.43 μg mL^{-1} using PDDA–MWCNTs–TiO_2NPs/PGE.

3.5. Interaction between methylene blue and ds-DNA via guanine and adenine oxidation

In order to investigate the efficiency of the prepared PDDA–MWCNTs–TiO_2NPs/PGE in the determination of the interaction between ds-DNA and small molecules, methylene blue was chosen as a model substance. The interaction between methylene blue and guanine base of ds-DNA is well known in the literature [34–36]. The difference in the oxidation signals of guanine base of ds-DNA in the presence and absence of small molecules is the basis for the preparation of DNA biosensors [37].

In order to investigate the effect of the interaction time between methylene blue and the ds-DNA on the oxidation peaks current of guanine and adenine bases, the experiments were performed using different interaction times in the presence of 6.40 μg mL^{-1} methylene blue. The oxidation peaks current obtained for guanine and adenine as a function of interaction time in the absence of methylene blue revealed that the values for the oxidation peaks current of guanine and adenine remained nearly unchanged in the absence of methylene blue. On the other hand, the oxidation peaks current of guanine and adenine gradually decreased with increasing interaction time up to 500 s in the presence of methylene blue beyond, which the oxidation peaks current did not change in spite of the increasing interaction time.

To compare the efficiencies of ds-DNA modified electrodes, the interaction of methylene blue with ds-DNA on the surface of PDDA–MWCNTs/PGE and PDDA–MWCNTs–TiO_2NPs/PGE was

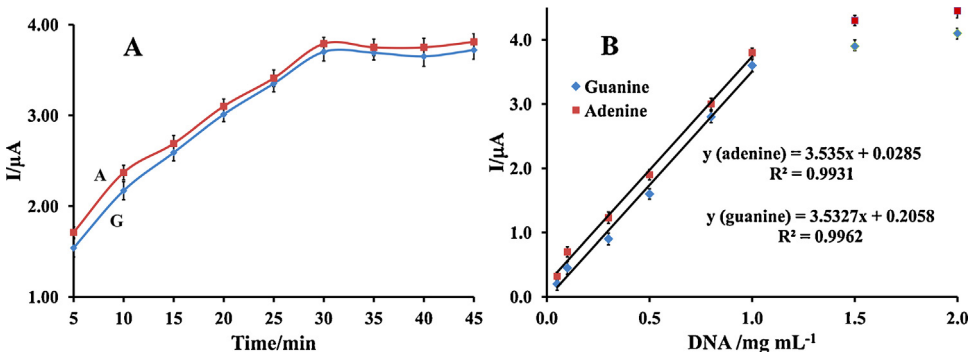

Fig. 5. (A) Effect of accumulation time of ds-DNA at PGE/PDDA–MWCNTs–TiO_2NPs/ds-DNA surface on the guanine and adenine oxidation signals. Conditions as in Fig. 2 with ds-DNA concentration of 1.0 mg mL^{-1}. (B) Effect of the ds-DNA concentration on the oxidation peaks current of guanine and adenine of the ds-DNA, obtained at PDDA–MWCNTs–TiO_2NPs/PGE. Other conditions are as Fig. 2. (The error bars are standard deviations for $n = 3$).

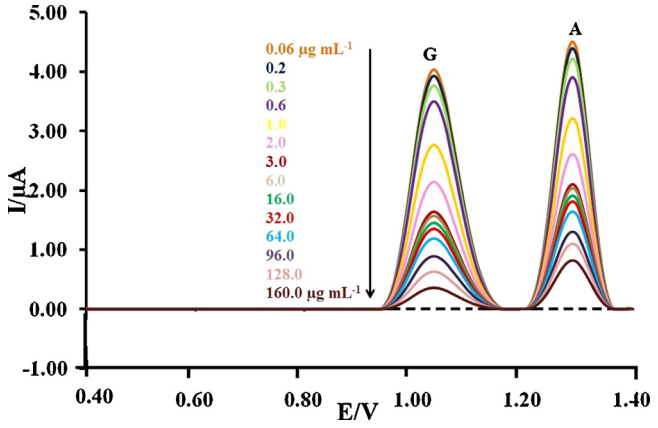

Fig. 6. Differential pulse voltammograms for the interaction of methylene blue with ds-DNA at the surface of PDDA–MWCNTs/PGE; oxidation signals of guanine and adenine after their interaction with methylene blue. The dashed line (– – –) represents the DPV of a bare PGE after incubation in 6.40 µg mL^{-1} methylene blue.

studied by DPV analysis, as shown in Figs. 6 and 7, respectively. Different concentrations of methylene blue were used to interact with the ds-DNA on the surface of the ds-DNA–modified PGE. It was found that the oxidation peaks current of guanine and adenine decreased with a concomitant increase in methylene blue concentration. A linear dependency was observed between the analytical signals (considered as the decrease in guanine and adenine signal before and after interaction with methylene blue)

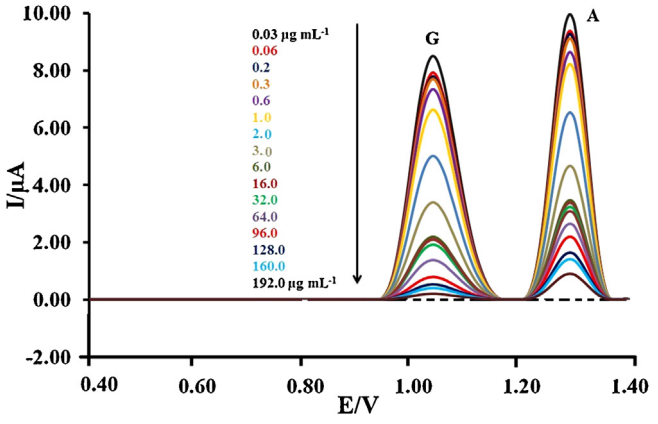

Fig. 7. Differential pulse voltammograms for the interaction of methylene blue with ds-DNA at the surface of PDDA–MWCNTs–TiO_2NPs/PGE; oxidation signals of guanine and adenine after their interaction with methylene blue. The dashed line (– – –) represents the DPV of a bare PGE after incubation in 6.40 µg mL^{-1} methylene blue.

Table 1
Stability data of the electrodes in the guanine signal measurement.

Electrode	Working stability (RSD%, $n = 4$)	Total stability (RSD%, $n = 10$)
DNA/MWCNT–PDDA/PGE	9.0	23.0
DNA/MWCNT–CHIT/PGE	10.0	27.0
ds-DNA/PDDA–TiO_2NPs/PGE	13.0	36.0
ds-DNA/chitosan–TiO_2NPs/PGE	11.0	33.0
ds-DNA/PDDA–MWCNTs–TiO_2NPs/PGE	5.0	9.0

and methylene blue concentrations in two regions for the both modified electrodes. Using DPV and following the changes in the oxidation signal intensity of guanine, after interaction with methylene blue (Figs. 6 and 7), the calibration curve was found to be linear in the range of 0.06–3.20 and 3.20–160.0 µg mL^{-1} methylene blue in the case of ds-DNA/PDDA-MWCNTs/PGE and 0.03–3.20 and 3.20–192.0 µg mL^{-1} methylene blue in the case of ds-DNA/PDDA–MWCNTs–TiO_2NPs/PGE. The limits of detection (LOD) of the proposed method, which equals $3S_b/m$ (where S_b is the standard deviation of the blank signal and m is the slope of the calibration curve), corresponded to 0.027 and 0.0038 µg mL^{-1} of methylene blue at the surface of ds-DNA/PDDA–MWCNTs/PGE and ds-DNA/PDDA–MWCNTs–TiO_2NPs/PGE, respectively.

3.6. Stability of the biosensor

Guanine signal measurement repeated within several days at the same biosensor was used to test the sensor stability. Between the measurements, the sensors were stored under dry conditions in an open air at room temperature. The working stability was characterized by a RSD value of the guanine peak current obtained from four consecutive measurements and the total stability was tested during a 20-day period by measuring the guanine signal every 3rd day. As can be seen from Table 1, the stability of the biosensor was improved in the case of ds-DNA/PDDA–MWCNTs–TiO_2NPs/PGE. Because DNA bases are attached rigidly to the MWCNTs and TiO_2NPs at the surface of ds-DNA/PDDA–MWCNTs–TiO_2NPs/PGE, the noise in the oxidation current measurements can be minimized. This improved stability can satisfy voltammetric assay of the interactions of the surface attached ds-DNA, as compared with the other electrodes.

4. Conclusions

A critical comparison of different strategies was presented for preparing DNA-based electrochemical nano-biosensors based on the dispersion of multiwall carbon nanotubes and titanium dioxide nanoparticles in polymeric matrices (PDDA and chitosan). To

compare different types of the modified electrodes used for DNA immobilization, a PGE modified with a mixture of MWCNTs and TiO_2NPs dispersed in PDDA was devised for the effective immobilization of DNA on graphite electrodes. PDDA–MWCNTs–TiO_2NPs modified electrode was shown to be an interesting support for DNA immobilization. The existence of both MWCNTs and TiO_2NPs was found to dramatically improve immobilization rates by covalent and electrostatic immobilization. Moreover, the storage stability of the immobilized DNA was found to be superior to those of conventional supports. Therefore, this support may be recommended as a new tool for DNA immobilization in DNA damage and interaction assays.

Acknowledgements

The authors wish to thank the Research Council of Isfahan University of Technology (IUT), the Center of Excellence in Sensor and Green Chemistry, and the Iranian Nanotechnology Initiative Council for their support.

References

[1] F.S. Nolte, B. Metchock, J.E. McGowan, A. Edwards, O. Okwumabua, C. Thurmond, P.S. Mitchell, B. Plikaytis, T. Shinnick, J. Clin. Microbiol. 31 (1993) 1777.
[2] S.R.A. Ferancova, Y. Kim, J. Labuda, M. Sillanpaa, Biosens. Bioelectron. 26 (2010) 314.
[3] M. Yamasuji, T. Shibata, T. Kabashima, M. Kai, Anal. Biochem. 413 (2011) 50.
[4] J. Li, W. Zhou, X. Ouyang, H. Yu, R. Yang, W. Tan, J. Yuan, Anal. Chem. 83 (2011) 1356.
[5] Y. Cheng, T. Stakenborg, P. Van Dorpe, L. Lagae, M. Wang, H. Chen, G. Borghs, Anal. Chem. 83 (2011) 1307.
[6] J. Zhang, L. Zhang, K. Zhou, X. Ye, C. Liu, J. Kang, C. Cai, Anal. Biochem. 413 (2011) 164.
[7] P. Du, H. Li, W. Cao, Biosens. Bioelectron. 24 (2009) 3223.
[8] Y. Xiao, R.Y. Lai, K.W. Plaxco, Nat. Protocol. 2 (2007) 2875.
[9] B. Moore, H. Hu, M. Singleton, F.M. De La Vega, M.G. Reese, M. Yandell, Genet. Med. 13 (2011) 210.
[10] S. Mansouri, Y. Cuie, F. Winnik, Q. Shi, P. Lavigne, M. Benderdour, E. Beaumont, J.C. Fernandes, Biomaterials 27 (2006) 2060.
[11] I. Palchetti, M. Mascini, Analyst 133 (2008) 846.
[12] X. Yang, Microbiology/Weishengwuxue Tongbao 37 (2010) 1227.
[13] P. Lonkar, P.C. Dedon, Int. J. Cancer 128 (2011) 1999.
[14] M. Mascini, I. Palchetti, G. Marrazza, Anal. Chem. 369 (2001) 15.
[15] S. Siddiquee, N.A. Yusof, A.B. Salleh, F. Abu Bakar, L.Y. Heng, Bioelectrochemistry 79 (2010) 31.
[16] J.J. Gooding, Electroanalysis 14 (2002) 1149.
[17] E. Palecek, F. Jelen, Crit. Rev. Anal. Chem. 3 (2002) 261.
[18] J. Wang, Trends Anal. Chem. 21 (2002) 226.
[19] K. Xu, J. Huang, Z. Ye, Y. Ying, Y. Li, Sensors 9 (2009) 5534.
[20] D. Samanta, A. Sarkar, Chem. Soc. Rev. 40 (2011) 2567.
[21] E.H. Lan, B. Dunn, J.I. Zink, Methods Mol. Biol. 300 (2005) 53.
[22] N.M. Dimitrijevic, Z.V. Saponjic, B.M. Rabatic, T. Rajh, J. Am. Chem. Soc. 127 (2005) 1344.
[23] Y.C. Zhang, T. Yang, N. Zhou, W. Zhang, K. Jiao, Sci. China (Ser. B) 51 (2008) 1066.
[24] H. Tang, F. Yan, Q. Tai, H.L.W. Chan, Biosens. Bioelectron. 25 (2010) 1646.
[25] A. Merkoçi, M. Pumera, X. Llopis, B. Perez, M. del Valle, S. Alegret, TRAC 24 (2005) 826.
[26] S. Rauf, J.J. Gooding, K. Akhtar, M.A. Ghauri, M. Rahman, M.A. Anwar, A.M. Khalid, J. Pharm. Biomed. Anal. 37 (2005) 205.
[27] R. Hajian, N. Shams, M. Mohagheghian, J. Braz. Chem. Soc. 20 (2009) 1399.
[28] A.A. Ensafi, E. Heydari-Bafrooei, Anal. Chem. 85 (2013) 991.
[29] A.A. Ensafi, M. Amini, B. Rezaei, Biosens. Bioelectron. 53 (2014) 43.
[30] D.J. Price, J.G. Joshi, J. Biol. Chem. 258 (1983) 10873.
[31] E. Casalino, C. Sblano, C. Landriscina, Arch. Biochem. Biophys. 346 (1997) 171.
[32] B. Halliwell, J.M.C. Gutteridge, Free Radicals in Biology and Medicine, third ed., Oxford University Press, 1999.
[33] A. Erdem, K. Kerman, B. Meric, M. Nzscz, Electroanalysis 13 (2001) 219.
[34] W. Yang, M. Özsöz, D.B. Hibbert, J.J. Gooding, Electroanalysis 14 (2002) 1299.
[35] P. Kara, K. Kerman, D. Ozkan, B. Meric, A. Erdem, Z. Ozkan, M. Özsöz, Electrochem. Commun. 4 (2002) 705.
[36] A. Erdem, K. Kerman, B. Meric, U.S. Akarca, M. Özsöz, Anal. Chim. Acta 422 (2000) 139.
[37] M.E. Ghica, R. Pauliukaite, O. Fatibello Filho, C.M.A. Brett, Sens. Actuators B 142 (2009) 308.
[38] A.A. Ensafi, E. Heydari-Bafrooei, B. Rezaei, Biosens. Bioelectron. 41 (2013) 627.
[39] P. Chen, R.L. McCreery, Anal. Chem. 68 (1996) 3958.
[40] A.A. Ensafi, M. Amini, B. Rezaei, Sens. Actuators B 177 (2013) 862.
[41] A.A. Ensafi, E. Heydari-bafrooei, M. Amini, Biosens. Bioelectron. 31 (2012) 376.
[42] A. Özcan, Y. Sahin, M. Özsöz, S. Turan, Electroanalysis 19 (2007) 2208.
[43] K.R. Meier, M. Gratzel, ChemPhysChem. 3 (2002) 371.
[44] S. Meng, E. Kaxiras, in: A. Merkoci (Ed.), Biosensing using Nanomaterials, John Wiley & Sons, Inc, 2009 (Chapter 3).